Neth Heart J (2012) 20:410–418
DOI 10.1007/s12471-012-0306-6

REVIEW ARTICLE

CT fractional flow reserve: the next level in non-invasive cardiac imaging

M. F. L. Meijs · M. J. Cramer · H. El Aidi · P. A. Doevendans

Published online: 24 July 2012

Abstract The haemodynamic effect of a coronary artery stenosis is a better predictor of prognosis than anatomical lumen obstruction. Until recently, no individual non-invasive test could provide both accurate coronary anatomy and lesion-specific myocardial ischaemia. However, computer tomography (CT) fractional flow reserve, which can be calculated from a standard CT coronary angiogram, was recently demonstrated to accurately detect and rule out the haemodynamic significance of individual coronary artery stenoses.

Keywords CT coronary angiography · Fractional flow reserve (FFR) · Non-invasive cardiac imaging · Single photon emission computed tomography (SPECT) · Positron emission tomography (PET) · Myocardial perfusion imaging

Background

As demonstrated by the FAME study, the prognosis of a coronary artery stenosis is predicted more accurately by its functional effect on myocardial perfusion than by the degree of anatomical arterial lumen obstruction [1]. Current guidelines emphasise that invasive coronary angiography (ICA) with the measurement of fractional flow reserve (FFR) is the reference standard to determine the haemodynamic significance of individual coronary artery stenoses (class 1A indication) [2, 3]. ICA and FFR are not without risk, as complications such as bleeding, arrhythmia, stroke, coronary artery dissection and myocardial infarction may occur [4]. Also, as many as 40 % of patients undergoing ICA do not have obstructive coronary artery disease (CAD) and will not require percutaneous coronary intervention (PCI) or coronary artery bypass grafting (CABG) [5]. Thus, there is a need for non-invasive imaging modalities to reduce the number of invasive examinations in order to reduce risks and costs.

M. F. L. Meijs · M. J. Cramer · H. El Aidi · P. A. Doevendans (✉)
Department of Cardiology, University Medical Centre Utrecht,
HP E03.511, Heidelberglaan 100,
3584 CX Utrecht, the Netherlands
e-mail: p.doevendans@umcutrecht.nl

Comparison with ICA

While some imaging techniques have focused on coronary anatomy, others have focused on myocardial perfusion. The diagnostic performance of the various modalities for the per-patient detection of at least 1 ≥ 50 % stenosis on ICA is listed in Table 1.

CT coronary angiography (CTCA) has evolved rapidly over the last decade [6]. Three multicentre studies and a number of single-centre studies enrolling a total of 1527 angina patients have demonstrated 64-slice CTCA to accurately rule out CAD (Table 1). The negative predictive value (NPV) on a per-patient basis is excellent, at approximately 95 % [6–8] with the single exception of the study by Miller et al. who reported a considerably lower value [9]. However, mainly due to over-estimation of highly calcified lesions the positive predictive value (PPV) is more modest: 64 – 92 % on a per-patient basis in the multicentre studies [7–9]. Single-centre studies on newer generation CT scanners, such as dual source CT scanners, show a similar diagnostic performance to the single-centre studies on 64-slice CTCA, yet at a lower radiation dose (Table 1) [10]. Due to the relatively high rate of false-positive findings, the current appropriate use criteria limit CTCA to patients without known CAD and a low to intermediate likelihood of CAD [11]. In these patient categories, CTCA is also cost-effective [12].

Table 1 Diagnostic performance of various non-invasive tests for the per-patient detection of at least 1≥50 % stenosis on invasive coronary angiography

Test	N	Sensitivity	Specificity	PPV	NPV	Accuracy	Reference
64-CTCA (single-centre, pooled)	646	98 %	88 %	94 %	95 %	94 %	Meijs [6]
64-CTCA (multi-centre)	360	99 %	64 %	86 %	97 %	88 %	Meijboom [8]
64-CTCA (multi-centre)	230	95 %	83 %	64 %	99 %	85 %	Budoff [7]
64-CTCA (multi-centre)	291	83 %	91 %	92 %	81 %	87 %	Miller [9]
DS-CTCA (single-centre, pooled)	764	97 %	89 %	90 %	97 %	93 %	Weustink [10]
MPI-SPECT (pooled)	4480	87 %	73 %	91 %	63 %	84 %	Klocke [22]
MPI-PET (pooled)	1660	90 %	89 %	94 %	73 %	90 %	Beanlands [21]
MPI-MR	676	82 %	86 %	79 %	88 %	*	Greenwood [33]
MPI-MR + MR coronary angiography	676	87 %	83 %	77 %	91 %	*	Greenwood [33]
MPI-SPECT + CTCA	130	99 %	87 %	91 %	98 %	84 %	Sato [45]

For CTCA, results of the single-centre studies on 64-slice CTCA (pooled estimate on original data), the 3 multicentre studies on 64-slice CTCA and the single-centre studies on dual-source CTCA (pooled estimate on original data) are presented separately

N number of patients, *CTCA* CT coronary angiography, *64-CTCA* 64-slice CTCA, *DS-CTCA* dual source CTCA, *MPI* myocardial perfusion imaging, *SPECT* single photon emission CT, *PET* positron emission tomography, *MR* magnetic resonance, *PPV* positive predictive value, *NPV* negative predictive value

* Accuracy was not reported for this study and could not be calculated from the presented data

Although the initial results of *magnetic resonance (MR) coronary angiography* have been encouraging, this technique is hampered by the relatively low spatial resolution of MR as compared with CT [13, 14]. Therefore, the present application of MR coronary angiography seems limited to the proximal and mid coronary segments.

Stress myocardial perfusion imaging (MPI) with single photon emission computed tomography (SPECT) [15], positron emission tomography (PET) [16] or MR [17, 18] and dobutamine cardiac MR stress imaging [19, 20] focus on the detection of regional myocardial ischaemia based on perfusion defects or wall motion abnormalities.

MPI-SPECT and MPI-PET have been extensively validated against ICA (Table 1) [21, 22]. While the PPV is high (91 %), the NPV is only modest (63 %). The performance of vasodilator stress MPI-SPECT compared with ICA is similar to exercise stress MPI-SPECT [22]. As a result of a higher spatial resolution, better attenuation correction and the ability of absolute quantification of myocardial flow, MPI-PET outperforms MPI-SPECT (Table 1), although larger direct comparative studies are lacking [16, 21, 23]. MPI-PET has a PPV of 94 % and an NPV of 73 % (Table 1). A normal MPI is associated with a favourable annual cardiac event rate of 0.6 % for MPI-SPECT [24] and 0.4–0.7 % for MPI-PET [25, 26].

In MPI-SPECT or relative perfusion PET, false-negative results due to 'balanced ischaemia' may occur in patients with multivessel or left-main CAD [27, 28]. In 143 patients with three-vessel disease on ICA, 18 % had no perfusion defect on MPI-SPECT [28]. Also, perfusion abnormalities were identified in all three coronary territories in only 46 % of these patients [28]. Similarly, in 101 patients with left-main CAD on ICA, >40 % of patients had low-risk findings on MPI-SPECT [27]. The ability of MPI-PET to enable absolute measurements of myocardial blood flow improves its sensitivity in left-main or multivessel disease [29–31]. In 103 angina patients with an intermediate pre-test risk for CAD, absolute quantification of myocardial perfusion with PET outperformed relative assessment of myocardial perfusion with PET [30]. The PPV improved from 61 % to 86 % and the NPV improved from 83 % to 97 % [30]. The addition of wall motion abnormalities and a decrease in left ventricular ejection fraction during stress resulted in a modest improvement of the detection and exclusion of three-vessel or left-main disease [27, 28, 32]. Also in this regard PET has the advantage over SPECT, as PET can measure peak rather than post-stress left ventricular ejection fraction [32].

Obesity may yield false-positive findings, although less frequently in MPI-PET than in MPI-SPECT, as MPI-PET has a higher spatial resolution and better attenuation correction [15]. Left-bundle block may give the false impression of septal perfusion defects [15].

MR myocardial perfusion imaging (MPI-MR) combined with wall motion analysis during adenosine stress and MR angiography has been compared with ICA and SPECT in 676 angina patients (Table 1) [33]. MPI-MRI with wall motion analysis had a fair NPV of 88 % but a modest PPV (79 %). The addition of MR coronary angiography did not markedly improve diagnostic performance (Table 1). MPI-MR outperformed MPI-SPECT, which had a PPV of 71 % and NPV of 79 % in this study. In a smaller study, *dobutamine stress MR* was demonstrated to have a similar diagnostic performance as MPI-MR compared with ICA [34].

Importantly, as no FFR measurements were performed in the above-mentioned studies, it may well be that some of the 'false-negative' findings of MPI compared with ICA actually represent haemodynamically non-significant lesions. The studies comparing MPI with FFR are discussed below.

Comparison with FFR

The correlation of CTCA and ICA with FFR is only moderate. In a study by Meijboom et al. in 79 stable angina patients, the diagnostic accuracy of quantitative CTCA and quantitative ICA to detect a haemodynamic lesion (here defined as FFR <75 %) on a per-vessel level was only 71 % and 67 %, respectively (Table 2) [35]. Koo et al. reported similar results (Table 2) [36]. However, in another study in 107 chest pain patients by Kajander et al. a markedly better diagnostic performance of CTCA compared with FFR was found, with an accuracy of 91 % (Table 2) [37]. This might be explained by the low prevalence of significant CAD (37 %) and multivessel CAD (21 %) by FFR in this study population. Koo and Kajander did not report the diagnostic performance of ICA to FFR.

The correlation of MPI-SPECT and FFR also seems only moderate, especially in multivessel disease (Table 2). In 36 patients with two- or three-vessel disease determined by FFR, 31 % of regions supplied by a vessel with an FFR-positive stenosis or occlusion had no perfusion defect on MPI-SPECT [38]. Accordingly, in two small studies by Forster et al. and Melikian et al. the NPV of MPI-SPECT compared with FFR in patients with angiographic two- or three-vessel disease was low (Table 2) [39, 40]. In the latter study, SPECT-MPI underestimated the number of ischaemic territories in 36 % of 67 patients [40]. Importantly, however, according to FFR no significant CAD was present in 20 of 67 patients, and only single-vessel CAD was present in another 20 of 67 patients [40].

In the aforementioned study by Kajander et al. MPI-PET had a PPV of 86 % and an NPV of 97 % on a per-patient level compared with FFR [37]. In a per-vessel analysis, the PPV was 78 % and the NPV was 98 % (Table 2). However, as mentioned above, the per-patient diagnostic performance of CTCA compared with FFR was also markedly higher in this study than in the studies by Meijboom et al. and Koo et al. Therefore, additional studies are required to determine the diagnostic performance of MPI-PET versus FFR.

MPI-MR and dobutamine stress MR (or the combination of these techniques) have been compared with FFR in three relatively small studies (42 to 103 patients) [41–43]. Although the reported PPV varies across these studies, the NPV is consistently high (Table 2). In a direct comparison, 3.0 T MPI-MR was found to be superior to 1.5 T MPI-MR for the detection of FFR-positive lesions [44]. In 1493 patients with known or suspected CAD, a negative dobutamine stress MR was associated with a <0.5 % 4-year event rate in patients with a low or intermediate pre-test probability of CAD [45]. However, the 4-year event rate in patients with a negative dobutamine stress MR but a high pre-test probability or with known CAD was still 5 % [45].

Combining anatomy and function

In conclusion, while CTCA has a high NPV but a modest PPV compared with ICA and FFR, the opposite holds true

Table 2 Diagnostic performance of various non-invasive tests for the per-vessel-territory detection of ischaemia (FFR<0.80*)

Test	N patients	Sensitivity	Specificity	PPV	NPV	Accuracy	Reference
ICA (quantitative)	79	57 %	69 %	49 %	76 %	65 %	Meijboom [35]
CTCA (quantitative)	79	45 %	79 %	54 %	73 %	67 %	Meijboom [35]
CTCA (visual)	79	94 %	48 %	49 %	43 %	64 %	Meijboom [35]
CTCA (visual)	107	75 %	95 %	76 %	94 %	91 %	Kajander [37]
CTCA (visual)	103	91 %	40 %	47 %	89 %	59 %	Koo [36]
MPI-SPECT	139	48–62 %	80–90 %	61–62 %	70–90 %	67–84 %	Forster [39], Melikian [40]
MPI-PET	107	95 %	92 %	78 %	98 %	92 %	Kajander [37]
MPI-MR	195	82 %–97 %	60–98 %	65–98 %	86–96 %	76–90 %	Kirschbaum [41], Watkins [43], *Lockie [42]
MPI-PET+CTCA	107	93 %	99 %	96 %	99 %	98 %	Kajander [37]
MPI-CT+CTCA	42	68 %	98 %	97 %	77 %	84 %	Ko [50]
CT-FFR	103	88 %	82 %	74 %	92 %	84 %	Koo [36]

The diagnostic performance on a per-vessel-territory level of various non-invasive tests for the detection of a stenosis with a fractional flow reserve (FFR) < 0.80 (*except for FFR < 0.75 in Lockie et al.)

As the reported diagnostic performance of the various tests varies considerably across studies, several CTCA studies have been listed separately and a range is reported for MPI-MR. Abbreviations as for Table 1. CT-FFR = CT fractional flow reserve

for MPI. MPI-PET and MPI-MR seem to correlate better with FFR than MPI-SPECT, although only limited data are available. Also, correlating a perfusion defect to a specific coronary artery stenosis can be challenging. As a logical next step, it was studied whether the combination of CTCA and MPI improves diagnostic performance.

In a study by Sato et al. in 130 angina patients, the combination of CTCA and MPI-SPECT improved the detection of significant CAD on ICA compared with CTCA alone [46]. The per-patient PPV increased from 82 % to 97 % without a decrease in NPV (Table 1).

Kajander et al. compared CTCA and CTCA combined with MPI-PET with invasive FFR in the aforementioned study in 107 stable angina patients [37]. Only vessels with both a≥50 % stenosis on CTCA and a perfusion defect on PET in the region of the vessel were classified as significantly stenosed. In a per-patient analysis, CTCA and MPI-PET alone each had a high NPV (97 %), but a more modest PPV (81 % and 86 %, respectively) compared with FFR. The combination of CTCA and MPI-PET resulted in a near-perfect PPV of 100 % and NPV of 98 % on a patient level. Similar excellent performance of CTCA combined with MPI-PET was found on a per-vessel level (Table 2). As mentioned above, in this study the diagnostic performance of CTCA versus FFR was higher than in other studies, possibly due to a low prevalence of CAD.

Technological advancements have enabled MPI with CT (MPI-CT) [47], for which a good correlation with MPI-SPECT was demonstrated [47]. In two studies in 45 and 35 angina patients, respectively, MPI-CT combined with CTCA had a PPV of 88 % and 86 % and an NPV of 91 % and 93 %, respectively, in a per-vessel analysis for the detection of≥ 50 % stenosis on ICA [48, 49]. In 42 patients with at least 1≥50 % angiographic stenosis on ICA, MPI-CT combined with CTCA was compared with invasive FFR by Ko et al. [50]. MPI-CT combined with CTCA had a PPV of 97 % and an NPV of 77 % in a per-vessel analysis compared with FFR (Table 2) [50]. In 33 patients, of whom 22 had a positive FFR value or a>85 % stenosis on ICA, MPI-CT combined with CTCA had a per-vessel PPV of 75 % and NPV of 97 % [51].

Preliminary data have indicated that the transluminal attenuation gradient may improve the accuracy of CTCA compared with ICA, especially in severely calcified lesions [52].

Although these new CT techniques and the combination of MPI-SPECT or MPI-PET with CTCA seem highly promising, larger studies and studies in patient populations with a higher prevalence of (multivessel) CAD are warranted.

CT-FFR

The application of computational fluid dynamics to CTCA has enabled the calculation of FFR values from standard CTCA scans without the need of additional medication, image acquisition or radiation exposure [53]. The recent DISCOVER-FLOW study comparing CT-FFR to invasive FFR demonstrates that CT-FFR accurately detects and rules out haemodynamically significant coronary artery stenosis [36].

Technical aspects

Technical aspects of CTCA

We have discussed the technical aspects of CTCA in more detail previously [6]. In brief, a multi-slice CT scanner contains an X-ray tube opposite a row of multiple thin detectors. A breath hold is required to prevent breathing artefacts. To synchronise for cardiac motion, image acquisition takes place in either a retrospective ECG-gated or prospective ECG-triggered fashion. Scanning the entire heart in one gantry rotation has become feasible with the 320-row CT scanner [54]. This renders CTCA less vulnerable to artefacts due to breathing, irregular heart rhythm or higher rate [54]. Also, temporal resolution has improved with faster gantry rotation times and the advent of dual source CT scanners [55], enabling the reconstruction of a cross-sectional image from a 90° instead of a 180° rotation. These improvements have led to modern CT protocols based on prospective ECG-triggered image acquisition (FLASH), which has resulted in a drastic reduction in radiation dose from 17 mSv to 1.5 mSv [56].

Technical aspects of FFR

The technical aspects of FFR have been discussed in more detail elsewhere by Pijls et al. [57]. FFR is the ratio of maximum blood flow in a stenotic artery to maximum blood flow if the same artery were normal [57]. Normal epicardial coronary arteries do not contribute significantly to the resistance in the total coronary network including the microvasculature. A larger amount of myocardial mass supplied by the vessel results in a larger maximal flow, and thus, in a larger pressure gradient over a given stenosis. Therefore, a given remaining coronary lumen area will result in a lower FFR if a larger myocardial mass is supplied by the vessel. Conversely, after a myocardial infarction, the amount of perfused myocardium decreases, and the FFR will increase. As the relation between myocardial blood flow and intracoronary pressure is linear during maximal hyperaemia, FFR can be calculated as the ratio of the coronary pressure distal to the stenosis and the mean aortic pressure during hyperaemia.

An intracoronary nitrate bolus is given to abolish epicardial vasoconstriction. During maximal hyperaemia induced by (e.g.) adenosine, intracoronary pressure distal to the stenosis is determined with a guide wire with an integrated pressure

sensor. Aortic pressure is taken as a reference to determine maximum blood flow if no stenosis would have been present.

As a result of the simultaneous measurement of aortic and intracoronary pressure, FFR is not influenced by changes in systemic haemodynamics. FFR also takes into account the (positive or negative) contribution of collaterals.

An FFR <0.75 was shown to be almost always associated with myocardial ischaemia [58]. Conversely, an FFR>0.80 was almost never associated with myocardial ischaemia [57]. For FFR values between 0.75 and 0.80 the association with ischaemia is less clear [57]. The FFR cut-offs hold true for patients with left-main or multivessel CAD, previous myocardial infarction or diabetes [57]. In sequential stenoses, a pull-back FFR measurement can be performed to appreciate the haemodynamic contribution of the individual stenoses. However, FFR measurement should not be performed within 5 days after acute myocardial infarction [57]. In the FAME study, FFR-guided intervention in multivessel disease decreased the incidence of adverse events by 30 % [1]. The risk of myocardial infarction or death associated with stenoses with an FFR>0.80 is approximately 1 % per year. PCI does not improve this prognosis [59].

Technical aspects of CT-FFR

CT-FFR is based on computational fluid dynamics. The equations used for computational fluid dynamics were formulated as early as the 19th century, based on the law of conservation of mass and balance of momentum. However, the solution of these equations only became possible with modern computing power and numerical methods.

Computational fluid dynamics is most widely known for its application in airplane and car design, e.g., for a given design of an airplane wing (‘the geometry’), the velocity and pressure of air around every point on that wing can be calculated based on the relative velocity of incoming air and atmospheric pressure (‘the boundary conditions’) and the viscosity and density of the air (‘the fluid properties’). Thus, lift and drag provided by that wing can be calculated.

The same principles can be applied to the coronary arteries [60]. First, a detailed analysis of coronary anatomy (‘the geometry’) is made based on CTCA. Next, the boundary conditions are calculated: mean aortic pressure, resting coronary flow and coronary microcirculatory resistance (and its reaction to maximal hyperaemia). Mean aortic pressure is estimated by measurement of blood pressure with a sphygmomanometer before CTCA. In the absence of acute myocardial ischaemia during CTCA, it can be assumed that resting coronary blood flow is proportional to myocardial mass [61]. Myocardial mass can be calculated accurately from CTCA [62]. The coronary microcirculatory resistance is assumed to be inversely (although not linearly) proportional to the size of the epicardial vessel [63]. Finally, the reaction of the microvasculature to adenosine is known to react predictably to maximal hyperaemia (adenosine) [64]. Viscosity and density of blood (‘the fluid properties’) are related to haematocrit values. Thus, velocity and pressure of blood in the coronaries are calculated. Thereby, for every point in the coronary arteries, FFR values can be calculated as the ratio of coronary pressure and mean aortic pressure (Fig. 1).

An even more advanced application would be the prediction of post-PCI CT-FFR. This is done by software-based removal of the stenosis (assuming an optimal result of the PCI) and re-calculating CT-FFR for the vessel without stenosis.

Radiation dose

Radiation exposure is a factor of concern in CT, SPECT and PET imaging. The combination of SPECT or PET perfusion with CTCA requires the patient to undergo two scans, resulting in increased radiation exposure and increased costs. A modern prospectively acquired CTCA has a modest radiation dose of 1.5 mSv [56]. The addition of CT perfusion to CTCA substantially increases the radiation dose to approximately 12 mSv [50]. Isolated rest and stress SPECT requires 11–12 mSv and isolated rest and stress PET requires 3 to 4 mSv [65]. The radiation dose for SPECT and PET combined with prospectively acquired CTCA is approximately 13 mSv [66] and 9.3 mSv [37], respectively. ICA is associated with a radiation dose of 7 mSv [37]. As standard CTCA scans are used, CT-FFR does not increase the radiation dose compared with CTCA.

The DISCOVER-FLOW study: CT-FFR versus invasive FFR

Recently, Koo et al. compared CTCA and CT-FFR to invasive FFR in the DISCOVER-FLOW study [36]. In this study, 103 stable angina patients were included who underwent ICA with FFR for clinical reasons and CTCA for study purposes. In order to be eligible, patients were required to have at least 1≥50 % stenosis on CTCA in a major coronary artery. Both patients with and without known CAD were included. The major exclusion criteria were life expectancy <2 years, contraindications to CTCA or medication required for CTCA or FFR, previous CABG or a non-evaluable CTCA. The study was powered on a per-vessel analysis. In this multivendor multicentre study, the radiation dose ranged from 3 mSv (for prospective scans) to 15 mSv (for retrospective scans). Stenoses on CTCA were visually classified as none (0 %), mild (1–49 %), moderate (50–69 %) or severe (≥ 70 %). CT-FFR values were calculated as described above. FFR was performed as clinically indicated. An invasive FFR<0.80 was considered diagnostic of lesion-specific ischaemia. In six vessels that were 99 % occluded, no FFR was performed for safety

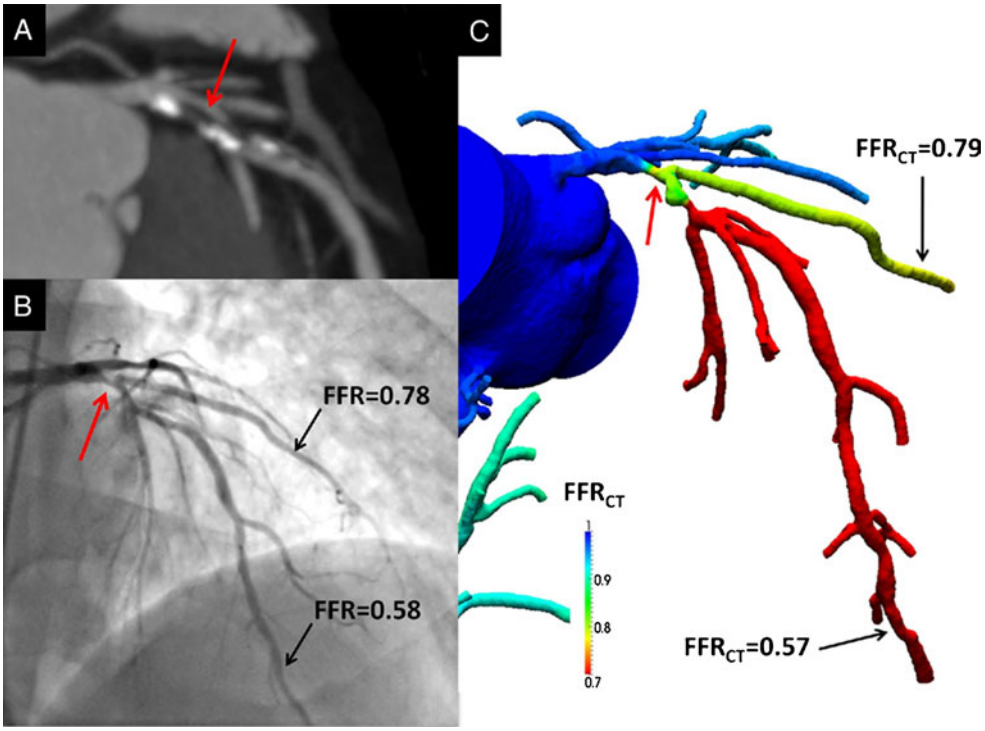

Fig. 1 Anatomically obstructive stenosis with a lesion causing ischaemia (**a**) Multiplanar reformat of coronary computed tomography angiography demonstrating obstructive (> 50 %) stenosis (*white arrow*) in the proximal portion of the left anterior descending (LAD) artery. (**b**) Invasive coronary angiography confirms the LAD stenosis (*red arrow*) with corresponding haemodynamically significant reductions in coronary pressure in the first diagonal branch (0.78) and distal LAD (0.58) by FFR. (**c**) Noninvasive computation of FFR from FFRCT of the first diagonal branch (0.79) and distal LAD (0.57), demonstrating lesion-specific ischaemia of the proximal LAD stenosis. (Reproduced with permission from Koo et al. J Am Coll Cardiol. 2011 [36])

reasons. Whereas in the FAME study subtotally occluded vessels were assigned an FFR value of 0.50 [1], in the current study these vessels were excluded from the analysis to prevent overestimation of the diagnostic performance of CT-FFR. The mean age of the patients was 62.7 years and 72 % of patients were male. Medical history included previous myocardial infarction or previous PCI in 17 % and 16 % of patients, respectively. The mean left ventricular ejection fraction was 62 %. As expected, the prevalence of cardiovascular risk factors and the use of cardiac medication was high.

Although the study was not powered on a per-patient level, CTCA had a per-patient PPV of 58 % and an NPV of 80 % compared with FFR. CT-FFR reduced the number of false positives, which resulted in a much higher PPV (85 %), without a decrease in NPV (81 %) compared with FFR. The addition of CTCA stenosis to CT-FFR did not improve the diagnostic performance. Also in a per-vessel comparison with FFR, the number of false-positive findings was much lower for CT-FFR than for CTCA, and hence the PPV was much higher for CT-FFR than for CTCA without a decrease in NPV (Table 2).

There were four false-negative lesions, all of which had an FFR value in the 'grey zone' between 0.75 and 0.80. Repeating the analyses with an FFR cut-off of 0.75 yielded similar results. Assigning an FFR value of 0.50 to subtotally occluded lesions further improved the performance of CT-FFR.

Future perspectives and studies

In the DeFACTO study, 238 patients will undergo CTCA, ICA and 3-vessel FFR in order to determine the diagnostic performance of CT-FFR compared with invasive FFR [67]. Patients, without prior PCI in the suspected culprit vessel and without prior CABG, who undergo CTCA and afterwards ICA for clinical reasons are eligible. CTCA will be performed on scanners with 64 or more detector rows. Stenosis with <30 % lumen narrowing on CTCA will be considered negative. For stenosis with≥30 % on CTCA, CT-FFR will be calculated. It is planned that up to 12 % of subjects will have unevaluable CTCA, ICA or FFR results. Study aims are per-patient and per-vessel diagnostic performance of CT-FFR compared with FFR. Also, as a secondary objective, the diagnostic accuracy of predicted post-PCI CT-FFR compared with post-PCI FFR will be assessed.

If the DeFACTO study results are positive, further studies are warranted to confirm that a ≥50 % stenosis on CTCA with a negative CT-FFR value is associated with an event-free follow-up. Also, the cost-effectiveness of CTCA with CT-FFR needs to be compared with regular clinical care and compared with CTCA without CT-FFR.

Conclusion

As CT-FFR seems to reduce the number of false-positive findings on CTCA by providing lesion-specific ischaemia,

this promising new technique may lead to a further reduction in inappropriate referrals for ICA. Also, CT-FFR may extend the use of CTCA to wider patient populations.

Conflict of interest None.

References

1. Pijls NH, Fearon WF, Tonino PA, et al. Fractional flow reserve versus angiography for guiding percutaneous coronary intervention in patients with multivessel coronary artery disease: 2-year follow-up of the FAME (fractional flow reserve versus angiography for multivessel evaluation) study. J Am Coll Cardiol. 2010;56:177–84.
2. Levine GN, Bates ER, Blankenship JC, et al. ACCF/AHA/SCAI guideline for percutaneous coronary intervention. A report of the American College of Cardiology Foundation/American Heart Association Task Force on Practice Guidelines and the Society for Cardiovascular Angiography and Interventions. J Am Coll Cardiol. 2011;58:e44–e122.
3. Wijns W, Kolh P, Danchin N, et al. Guidelines on myocardial revascularization. Eur Heart J. 2010;31:2501–55.
4. Noto Jr TJ, Johnson LW, Krone R, et al. Cardiac catheterization 1990: a report of the Registry of the Society for Cardiac Angiography and Interventions (SCA&I). Catheter Cardiovasc Diagn. 1991;24:75–83.
5. Patel MR, Peterson ED, Dai D, et al. Low diagnostic yield of elective coronary angiography. N Engl J Med. 2010;362:886–95.
6. Meijs MF, Meijboom WB, Cramer MJ, et al. Computed tomography of the coronary arteries: an alternative? Scand Cardiovasc J. 2007;41:277–86.
7. Budoff MJ, Dowe D, Jollis JG, et al. Diagnostic performance of 64-multidetector row coronary computed tomographic angiography for evaluation of coronary artery stenosis in individuals without known coronary artery disease: results from the prospective multicenter ACCURACY (assessment by coronary computed tomographic angiography of individuals undergoing invasive coronary angiography) trial. J Am Coll Cardiol. 2008;52:1724–32.
8. Meijboom WB, Meijs MF, Schuijf JD, et al. Diagnostic accuracy of 64-slice computed tomography coronary angiography: a prospective, multicenter, multivendor study. J Am Coll Cardiol. 2008;52:2135–44.
9. Miller JM, Rochitte CE, Dewey M, et al. Diagnostic performance of coronary angiography by 64-row CT. N Engl J Med. 2008;359:2324–36.
10. Weustink AC, de Feyter PJ. The role of multi-slice computed tomography in stable angina management: a current perspective. Neth Heart J. 2011;19:336–43.
11. Taylor AJ, Cerqueira M, Hodgson JM, et al. ACCF/SCCT/ACR/AHA/ASE/ASNC/NASCI/SCAI/SCMR 2010 appropriate use criteria for cardiac computed tomography. A report of The American College of Cardiology Foundation Appropriate Use Criteria Task Force, the Society of Cardiovascular Computed Tomography, the American College of Radiology, the American Heart Association, the American Society of Echocardiography, the American Society of Nuclear Cardiology, the North American Society for Cardiovascular Imaging, the Society for Cardiovascular Angiography and Interventions, and the Society for Cardiovascular Magnetic Resonance. J Am Coll Cardiol. 2010;56:1864–94.
12. Genders TS, Meijboom WB, Meijs MF, et al. CT coronary angiography in patients suspected of having coronary artery disease: decision making from various perspectives in the face of uncertainty. Radiology. 2009;253:734–44.
13. Kato S, Kitagawa K, Ishida N, et al. Assessment of coronary artery disease using magnetic resonance coronary angiography: a national multicenter trial. J Am Coll Cardiol. 2010;56:983–91.
14. Kim WY, Danias PG, Stuber M, et al. Coronary magnetic resonance angiography for the detection of coronary stenoses. N Engl J Med. 2001;345:1863–9.
15. Beller GA, Heede RC. SPECT imaging for detecting coronary artery disease and determining prognosis by noninvasive assessment of myocardial perfusion and myocardial viability. J Cardiovasc Transl Res. 2011;4:416–24.
16. Schindler TH, Schelbert HR, Quercioli A, et al. Cardiac PET imaging for the detection and monitoring of coronary artery disease and microvascular health. JACC Cardiovasc Imaging. 2010;3:623–40.
17. Ishida N, Sakuma H, Motoyasu M, et al. Noninfarcted myocardium: correlation between dynamic first-pass contrast-enhanced myocardial MR imaging and quantitative coronary angiography. Radiology. 2003;229:209–16.
18. Sakuma H, Suzawa N, Ichikawa Y, et al. Diagnostic accuracy of stress first-pass contrast-enhanced myocardial perfusion MRI compared with stress myocardial perfusion scintigraphy. AJR Am J Roentgenol. 2005;185:95–102.
19. Kitagawa K, Sakuma H, Nagata M, et al. Diagnostic accuracy of stress myocardial perfusion MRI and late gadolinium-enhanced MRI for detecting flow-limiting coronary artery disease: a multicenter study. Eur Radiol. 2008;18:2808–16.
20. de Mello RA, Nacif MS, Dos Santos AA, et al. Diagnostic performance of combined cardiac MRI for detection of coronary artery disease. Eur J Radiol. 2011.
21. Beanlands RS, Youssef G. Diagnosis and prognosis of coronary artery disease: PET is superior to SPECT: Pro. J Nucl Cardiol. 2010;17:683–95.
22. Klocke FJ, Baird MG, Lorell BH, et al. ACC/AHA/ASNC guidelines for the clinical use of cardiac radionuclide imaging–executive summary: a report of the American College of Cardiology/American Heart Association Task Force on Practice Guidelines (ACC/AHA/ASNC Committee to Revise the 1995 Guidelines for the Clinical Use of Cardiac Radionuclide Imaging). Circulation. 2003;108:1404–18.
23. Go RT, Marwick TH, MacIntyre WJ, et al. A prospective comparison of rubidium-82 PET and thallium-201 SPECT myocardial perfusion imaging utilizing a single dipyridamole stress in the diagnosis of coronary artery disease. J Nucl Med. 1990;31:1899–905.
24. Shaw LJ, Iskandrian AE. Prognostic value of gated myocardial perfusion SPECT. J Nucl Cardiol. 2004;11:171–85.
25. Yoshinaga K, Chow BJ, Williams K, et al. What is the prognostic value of myocardial perfusion imaging using rubidium-82 positron emission tomography? J Am Coll Cardiol. 2006;48:1029–39.
26. Dorbala S, Hachamovitch R, Curillova Z, et al. Incremental prognostic value of gated Rb-82 positron emission tomography myocardial perfusion imaging over clinical variables and rest LVEF. JACC Cardiovasc Imaging. 2009;2:846–54.
27. Berman DS, Kang X, Slomka PJ, et al. Underestimation of extent of ischemia by gated SPECT myocardial perfusion imaging in patients with left main coronary artery disease. J Nucl Cardiol. 2007;14:521–8.
28. Lima RS, Watson DD, Goode AR, et al. Incremental value of combined perfusion and function over perfusion alone by gated SPECT myocardial perfusion imaging for detection of severe three-vessel coronary artery disease. J Am Coll Cardiol. 2003;42:64–70.
29. Parkash R, de Kemp RA, Ruddy TD, et al. Potential utility of rubidium 82 PET quantification in patients with 3-vessel coronary artery disease. J Nucl Cardiol. 2004;11:440–9.
30. Kajander SA. Clinical value of absolute quantification of myocardial perfusion with (15)O-water in coronary artery disease. Circ Cardiovasc Imaging. 2011;4:678–84.

31. Hajjiri MM, Leavitt MB, Zheng H, et al. Comparison of positron emission tomography measurement of adenosine-stimulated absolute myocardial blood flow versus relative myocardial tracer content for physiological assessment of coronary artery stenosis severity and location. JACC Cardiovasc Imaging. 2009;2:751–8.
32. Dorbala S, Vangala D, Sampson U, et al. Value of vasodilator left ventricular ejection fraction reserve in evaluating the magnitude of myocardium at risk and the extent of angiographic coronary artery disease: a 82Rb PET/CT study. J Nucl Med. 2007;48:349–58.
33. Greenwood JP, Maredia N, Younger JF, et al. Cardiovascular magnetic resonance and single-photon emission computed tomography for diagnosis of coronary heart disease (CE-MARC): a prospective trial. Lancet. 2012;379:453–60.
34. Paetsch I, Jahnke C, Wahl A, et al. Comparison of dobutamine stress magnetic resonance, adenosine stress magnetic resonance, and adenosine stress magnetic resonance perfusion. Circulation. 2004;110:835–42.
35. Meijboom WB, van Mieghem CA, van Pelt N, et al. Comprehensive assessment of coronary artery stenoses: computed tomography coronary angiography versus conventional coronary angiography and correlation with fractional flow reserve in patients with stable angina. J Am Coll Cardiol. 2008;%19;52:636–43.
36. Koo BK, Erglis A, Doh JH, et al. Diagnosis of ischemia-causing coronary stenoses by noninvasive fractional flow reserve computed from coronary computed tomographic angiograms. Results from the prospective multicenter DISCOVER-FLOW (diagnosis of ischemia-causing stenoses obtained Via noninvasive fractional flow reserve) study. J Am Coll Cardiol. 2011;58:1989–97.
37. Kajander S, Joutsiniemi E, Saraste M, et al. Cardiac positron emission tomography/computed tomography imaging accurately detects anatomically and functionally significant coronary artery disease. Circulation. 2010;122:603–13.
38. Ragosta M, Bishop AH, Lipson LC, et al. Comparison between angiography and fractional flow reserve versus single-photon emission computed tomographic myocardial perfusion imaging for determining lesion significance in patients with multivessel coronary disease. Am J Cardiol. 2007;99:896–902.
39. Forster S. Tc-99 m sestamibi single photon emission computed tomography for guiding percutaneous coronary intervention in patients with multivessel disease: a comparison with quantitative coronary angiography and fractional flow reserve. Int J Cardiovasc Imaging. 2010;26:203–13.
40. Melikian N, De Bondt P, Tonino P, et al. Fractional flow reserve and myocardial perfusion imaging in patients with angiographic multivessel coronary artery disease. JACC Cardiovasc Interv. 2010;3:307–14.
41. Kirschbaum SW, Springeling T, Rossi A, et al. Comparison of adenosine magnetic resonance perfusion imaging with invasive coronary flow reserve and fractional flow reserve in patients with suspected coronary artery disease. Int J Cardiol. 2011;147:184–6.
42. Lockie T, Ishida M, Perera D, et al. High-resolution magnetic resonance myocardial perfusion imaging at 3.0-Tesla to detect hemodynamically significant coronary stenoses as determined by fractional flow reserve. J Am Coll Cardiol. 2011;57:70–5.
43. Watkins S, Lyne J, Steedman T, et al. Validation of magnetic resonance myocardial perfusion imaging with fractional flow reserve for the detection of significant coronary heart disease. Circulation. 2009;120:2207–13.
44. Bernhardt P, Walcher T, Rottbauer W, et al. Quantification of myocardial perfusion reserve at 1.5 and 3.0 Tesla: a comparison to fractional flow reserve. Int J Cardiovasc Imaging. 2012.
45. Korosoglou G, Elhmidi Y, Steen H, et al. Prognostic value of high-dose dobutamine stress magnetic resonance imaging in 1493 consecutive patients: assessment of myocardial wall motion and perfusion. J Am Coll Cardiol. 2010;56:1225–34.
46. Sato A, Nozato T, Hikita H, et al. Incremental value of combining 64-slice computed tomography angiography with stress nuclear myocardial perfusion imaging to improve non-invasive detection of coronary artery disease. J Nucl Cardiol. 2010;17:19–26.
47. Techasith T. Cury RC Stress myocardial CT perfusion: an update and future perspective. JACC Cardiovasc Imaging. 2011;4:905–16.
48. Ko SM, Choi JW, Hwang HK, et al. Diagnostic performance of combined noninvasive anatomic and functional assessment with dual-source CT and adenosine-induced stress dual-energy CT for detection of significant coronary stenosis. AJR Am J Roentgenol. 2012;198:512–20.
49. Rocha-Filho JA, Blankstein R, Shturman LD, et al. Incremental value of adenosine-induced stress myocardial perfusion imaging with dual-source CT at cardiac CT angiography. Radiology. 2010;254:410–9.
50. Ko BS, Meredith IT, Leung M, et al. Computed tomography stress myocardial perfusion imaging in patients considered for revascularization: a comparison with fractional flow reserve. Eur Heart J. 2012;33:67–77.
51. Bamberg F, Becker A, Schwarz F, et al. Detection of hemodynamically significant coronary artery stenosis: incremental diagnostic value of dynamic CT-based myocardial perfusion imaging. Radiology. 2011;260:689–98.
52. Choi JH, Min JK, Labounty TM, et al. Intracoronary transluminal attenuation gradient in coronary CT angiography for determining coronary artery stenosis. JACC Cardiovasc Imaging. 2011;4:1149–57.
53. Kim HJ, Vignon-Clementel IE, Coogan JS, et al. Patient-specific modeling of blood flow and pressure in human coronary arteries. Ann Biomed Eng. 2010;38:3195–209.
54. Uehara M, Takaoka H, Kobayashi Y, et al. Diagnostic accuracy of 320-slice computed-tomography for detection of significant coronary artery stenosis in patients with various heart rates and heart rhythms compared with conventional coronary-angiography. Int J Cardiol. 2012.
55. Leber AW, Johnson T, Becker A, et al. Diagnostic accuracy of dual-source multi-slice CT-coronary angiography in patients with an intermediate pretest likelihood for coronary artery disease. Eur Heart J. 2007;28:2354–60.
56. Srichai MB, Lim RP, Donnino R, et al. Low-dose, prospective triggered high-pitch spiral coronary computed tomography angiography: comparison with retrospective spiral technique. Acad Radiol. 2012;19:554–61.
57. Pijls NH, Sels JW. Functional measurement of coronary stenosis. J Am Coll Cardiol. 2012;59:1045–57.
58. Pijls NH, De Bruyne B, Peels K, et al. Measurement of fractional flow reserve to assess the functional severity of coronary-artery stenoses. N Engl J Med. 1996;334:1703–8.
59. Pijls NH, van Schaardenburgh P, Manoharan G, et al. Percutaneous coronary intervention of functionally nonsignificant stenosis: 5-year follow-up of the DEFER study. J Am Coll Cardiol. 2007;49:2105–11.
60. Zhou Y, Kassab GS, Molloi S. In vivo validation of the design rules of the coronary arteries and their application in the assessment of diffuse disease. Phys Med Biol. 2002;47:977–93.
61. Kamiya A, Togawa T. Adaptive regulation of wall shear stress to flow change in the canine carotid artery. Am J Physiol. 1980;239:H14–21.
62. Takx RA, Moscariello A, Schoepf UJ, et al. Quantification of left and right ventricular function and myocardial mass: comparison of low-radiation dose 2nd generation dual-source CT and cardiac MRI. Eur J Radiol. 2012;81:e598–604.

63. Zarins CK, Zatina MA, Giddens DP, et al. Shear stress regulation of artery lumen diameter in experimental atherogenesis. J Vasc Surg. 1987;5:413–20.
64. Wilson RF, Wyche K, Christensen BV, et al. Effects of adenosine on human coronary arterial circulation. Circulation. 1990;82:1595–606.
65. Di Carli MF, Murthy VL. Cardiac PET/CT for the evaluation of known or suspected coronary artery disease. Radiographics. 2011;31:1239–54.
66. George RT, Arbab-Zadeh A, Miller JM, et al. Computed tomography myocardial perfusion imaging with 320-Row detector CT accurately detects myocardial ischemia in patients with obstructive coronary artery disease. Circ Cardiovasc Imaging. 2012;1:330–40.
67. Min JK, Berman DS, Budoff MJ, et al. Rationale and design of the DeFACTO (determination of fractional flow reserve by anatomic computed tomographic AngiOgraphy) study. J Cardiovasc Comput Tomogr. 2011;5:301–9.